seeds

MDPI

Article

Seed Endophyte *Bacillus atrophaeus* Colonizes Root and Shoot Tissues Providing Antifungal Activity During Wheat Seedling Establishment

Anagha Wankhade [1], Zhiting Xu [2], Ashlynn Clark [1] and David Britt [1,*]

[1] Department of Biological Engineering, Utah State University, Logan, UT 84322, USA; anagha.wankhade@usu.edu (A.W.); ashlynn.clark@usu.edu (A.C.)
[2] College of Science, University of Utah, Salt Lake City, UT 84112, USA; zhitingxu052@gmail.com
* Correspondence: david.britt@usu.edu

Abstract

Seed-associated endophytes become active during germination, playing important roles as early colonizers of plant tissues and contributing to plant health while residing in a protective niche. In this study, we characterized a wheat-derived bacterial isolate, JunSE1L, to determine its functional traits and ecological role in the plant microbiome. The isolate was identified as *Bacillus atrophaeus* based on 16S rRNA analysis. JunSE1L exhibited nutrient-dependent plasticity in colony architecture, forming robust hydrophobic biofilms and pellicles under rich nutrient availability while swarming and forming thin, often dendritic colonies under defined nutrition. JunSE1L produced highly surface-active compounds that lowered the surface tension of water to 30 mN/m and released potent proteolytic and hemolytic compounds, thus equipping JunSE1L for antagonistic interactions, as examined against several fungal pathogens. JunSE1L inhibited *Fusarium proliferatum* and *Mucor hiemalis* in live-cell assays, while cell-free supernatant selectively inhibited *M. hiemalis*. JunSE1L was recovered from multiple plant compartments, including rhizosphere, rhizoplane, and aerial tissues, and was observed to emerge from cut plant tissues, supporting seed-endophyte mobilization upon germination to colonize distal tissues. Seed surface inoculation experiments with JunSE1L showed limited attachment at low cell densities and reduced seedling vigor at higher inoculum levels, indicating that inoculum density and native microbiome interactions influence seedling performance.

Keywords: *Bacillus atrophaeus*; seed endophyte; wheat microbiome; seed-to-surface transition; biofilm formation; antifungal activity; rhizosphere colonization; biosurfactant; biological control

Academic Editor: Aria Dolatabadian

Received: 21 March 2026
Revised: 22 May 2026
Accepted: 22 May 2026
Published: 26 May 2026

1. Introduction

Seed-associated endophytes are important contributors to early plant microbiome assembly and seedling establishment. Because they are already present at germination, these microorganisms can colonize emerging roots and shoots and influence microbial community development during early plant growth. Seed endophytes can also persist throughout the plant life cycle and may be transmitted across plant generations through both vertical and horizontal transmission routes, thereby shaping plant-associated microbiomes over time [1–3]. Consequently, seed-associated microbial communities represent an important reservoir of early colonizers. These microbes can influence plant health, stress

tolerance, and interactions with surrounding microbial communities. As such, they have been proposed as a potential sustainable alternative to agrochemical inputs.

Members of the genus *Bacillus* are among the most frequently recovered seed-borne and plant-associated bacteria across diverse crops, including cereals and quinoa [4–6]. Their success in plant-associated environments is partially attributed to the formation of stress-resistant endospores, which allow survival under desiccation, nutrient limitation, and temperature fluctuations typical of soil and aerial plant habitats [7,8]. In addition, many plant-associated *Bacillus* strains produce extracellular hydrolytic enzymes and membrane-active lipopeptides such as surfactin, iturin, and fengycin. These metabolites contribute to microbial competition and suppression of plant pathogens through mechanisms including antibiosis, niche competition, and activation of plant defense responses [9–12].

Successful colonization of plant surfaces requires adaptation to highly heterogeneous environmental conditions. The rhizosphere and phyllosphere exhibit strong spatial and temporal variation in nutrient availability, moisture, and abiotic stress, which shapes associated microbial communities [13,14]. In *Bacillus*, environmental conditions such as nutrient composition, osmotic stress, temperature, and water potential regulate colony architecture, extracellular matrix production, biofilm formation, and sporulation. Changes in nutrient availability or polymeric substrates can alter biofilm structure, hydrophobicity, and colony morphology, while osmotic stress can shift populations between motile and sessile states [15–17]. Biofilm development—including pellicle formation at the air-liquid interface—enhances persistence, surface attachment, and tolerance to environmental stress by embedding cells within an extracellular polymeric matrix [18,19]. Biosurfactants such as surfactin reduce surface tension and facilitate spreading motility, thus promoting stable colonization of plant surfaces and the induction of systemic resistance (ISR) in plants [15,20–22]. Biosurfactants also interact with hydrophobic interfaces, including air–water boundaries, and may influence interfacial processes relevant to xylem function [23]; however, their direct role in preventing xylem embolism remains to be established [24].

Through their persistence on plant surfaces, many plant-associated *Bacillus* strains contribute to plant health through direct antifungal activity. This antagonism is commonly mediated by secreted lipopeptides and related metabolites that disrupt fungal membranes, inhibit spore germination and hyphal growth, and suppress disease development in plants [25,26]. Lipopeptides such as iturins, fengycins, bacillomycins, and mycosubtilin can damage fungal membranes by altering ergosterol-dependent membrane integrity, causing leakage of cellular contents and growth inhibition. These properties underpin broad-spectrum suppression of phytopathogenic fungi and have led to the widespread use of *Bacillus*-based formulations as biological control agents in agriculture [27–29].

Despite the well-recognized role of *Bacillus* in plant health, most mechanistic studies have focused on rhizosphere-derived isolates or on individual functional traits examined in isolation, such as lipopeptide production or enzymatic activity [30]. In contrast, less attention has been given to how multiple adaptive traits operate together within a single seed-derived isolate. These traits include nutrient-dependent developmental plasticity, biofilm formation, biosurfactant production, persistence strategies, and antifungal activity. Understanding how these traits collectively enable seed endophytes to transition from seed-associated microbes to active plant surface colonizers remains an important gap in our understanding of plant–microbe interactions.

Crop yields are often compromised by abiotic stress (e.g., drought) that often increases plant susceptibility to biotic stressors, such as fungal pathogens. This study focused on two ecologically distinct fungal targets: *Fusarium proliferatum* and *Mucor hiemalis*. *Fusarium* species are among the most important fungal pathogens affecting cereal crops and are associated with seedling disease, root and crown rot, and mycotoxin contamination. In

contrast, *Mucor* species are fast-growing saprophytic fungi commonly found in soil and plant-associated environments. Testing antagonism against both organisms, therefore allows evaluation of bacterial antifungal activity across distinct fungal groups relevant to both plant pathology and soil microbial communities.

In this study, a bacterial endophyte was isolated from surface-sterilized wheat seeds and designated JunSE1L (Juniper Seed Endophyte isolate 1, large-colony variant). Preliminary phenotypic characteristics suggested affiliation with the genus *Bacillus*. We hypothesized that a seed-derived isolate exhibiting strong environmental plasticity and surface-associated traits could transition into a functional epiphyte with antifungal potential. To test this hypothesis, we (i) identified the isolate using 16S rRNA gene sequencing, (ii) evaluated its ability to colonize wheat root and shoot surfaces, (iii) characterized nutrient-dependent phenotypic plasticity and persistence-related traits—including colony architecture, hydrophobicity, biofilm and pellicle formation, sporulation, extracellular enzyme production, and biosurfactant activity—and (iv) assessed antifungal activity against *Fusarium proliferatum* and *Mucor hiemalis*. Together, these experiments were designed to determine whether a seed-borne *Bacillus* isolate can transition into a plant-associated surface colonizer with traits relevant to biological control.

2. Materials and Methods

2.1. Endophyte Isolation

Seeds of winter wheat (Triticum aestivum, var. Juniper, developed by the Idaho Agriculture Experiment Station as a stress-tolerant cultivar (https://digitalcommons.usu.edu/grcanyon/235/ (accessed on 23 May 2026)), collected from a 2020 organically grown harvest, were surface sterilized by immersion in 100 mL of 10% hydrogen peroxide (H_2O_2) (Sigma-Aldrich, Cat. No. 516813, MilliporeSigma, St. Louis, MO, USA) in 250 mL for 10 min with constant shaking. Seeds were added in a single layer covering the bottom of the flask to ensure uniform exposure to the sterilizing solution. After washing three times in sterile distilled water, five seeds were placed per plate on 2% Lysogeny Broth (LB) agar plates, with a total of eleven plates (n = 55 seeds, biological replicates). The plates were sealed with Parafilm™ and incubated at 22 °C for 4 d. Inoculum from a single colony growing around the surface of the wheat seeds was transferred into sterile water and serial dilutions were plated onto 2% LB agar. Purification of the single colonies growing on these plates utilized the three-streak method, which produced two stable cultures that yielded either large or small colonies when grown on 2% LB. These cultures were termed JunSE1L for the large colony form and JunSE1S for the small colony cell type. Cells were maintained in 15% glycerol at −75 °C. The studies in this paper involved the endophyte JunSE1L, which is the large colony phenotype.

2.2. Colonization of Wheat Roots and Shoots by Seed Endophyte JunSE1L

2.2.1. Seed Surface Sterilization and Plant Growth

Wheat seeds were surface sterilized by immersion in 10% H_2O_2, same as explained above, followed by three rinses with sterile distilled water. To verify the effectiveness of sterilization, seeds were placed on LB (2% agar; medium consisted of tryptone (Fisher BioReagents, Cat. No. BP1421; Fisher Scientific, Fair Lawn, NJ, USA), yeast extract (Fisher BioReagents, Cat. No. BP1422; Fisher Scientific, Fair Lawn, NJ, USA), and no added salt) plates and incubated for 24 h to check for microbial growth.

Magenta™ boxes (GA-7 plant culture vessels; Magenta LLC, Chicago, IL, USA) were prepared using sterile sand (Granusil 4075; Covia Solutions Inc., Emmett, ID, USA). Sand was washed and dry-sterilized at 200 °C for 14 h. 20 × 6 × 6 cm Magenta ™ boxes were disinfected with 70% ethanol, filled with 300 g sterile sand, and supplemented with 50 mL

sterile distilled water. The sand was mixed and fluffed using ethanol-sterilized tools before sowing. Surface-sterilized seeds, with no visible surface microbial growth, were planted in Magenta™ plant growth boxes (3 seeds/box) and grown for 6 days at 22 °C.

2.2.2. Assessment of Rhizosphere, Rhizoplane, and Phyllosphere Colonization

After 6 days, plants were harvested under sterile conditions in a biosafety cabinet. Seedlings were transferred onto sterile aluminum foil for processing.

Rhizosphere colonization: Sand adhering to roots was collected and transferred into sterile 15 mL tubes. Sterile distilled water was added at a ratio of 1 mL per 0.1 g sand and vortexed. 100 µL suspensions were plated onto LB (2% agar) to observe any bacterial growth.

Rhizoplane colonization: Roots were immersed in 10 mL sterile distilled water and vortexed for 1 min to detach surface-associated bacteria. 100 µL of the root wash was plated onto LB (2% agar). In addition, root segments were excised, gently cleaned of residual sand using sterile forceps, and placed directly onto LB plates to assess bacterial emergence from root tissues.

Phyllosphere colonization: Leaves were cut and plated directly onto LB (2% agar) plates to determine bacterial emergence from internal tissues.

All plates were incubated at 22 °C and monitored for colony development. Colony morphology was used as a preliminary indicator of strain identity when recovering bacteria from plant tissues, and molecular identification of the recovered bacteria was subsequently performed as described in Section 2.4.8.

2.3. Endophyte Emergence from Cut Plant Tissues on Agar

Surface-sterilized seeds (as described above) were placed directly onto 2% LB agar plates and incubated at 22 °C under sealed conditions (Parafilm™; Amcor Flexibles North America, Neenah, WI, USA). Seedlings were allowed to grow for five days without transferring to sand systems.

On day 5, roots and shoots were aseptically cut using 70% ethanol-sterilized tweezers inside a biosafety cabinet. Plates were resealed and returned to incubation at 22 °C. Emergence of bacterial colonies from the cut ends of plant tissues was monitored over time, and images were captured at regular intervals to document endophyte growth.

2.4. Characterization of Endophyte JunSE1L for the Production of Bacillus sp. Traits

The isolate JunSE1L was examined for its production of features characteristic of authentic *Bacillus* isolates. Traits examined were production of surfactants [31], hydrophobin [32–34], and spores, as well as hemolysis [35] and extracellular protease [36] activities.

2.4.1. Production of Hydrophobin and Spores

Hydrophobin production was assessed with colonies formed on LB or MM 2% agar surfaces. Mature colonies of JunSE1L were established by inoculation of the agar plates with 10 µL of stationary phase cells (OD_{600} of 0.5) suspended in sterile distilled water. These cells, from cultures grown in LB or MM broths to the stationary phase with shaking at 140 rpm at 22 °C, were pelleted by centrifugation and resuspended in sterile distilled water. These sealed agar plate cultures were incubated for 15 d, and then a 5 µL drop of distilled water was placed on a colony. Images of the drop were taken within a minute. The stability of the drop was timed up to 2 h.

Spore production was studied by staining using the Schaeffer-Fulton technique [37]. Briefly, a bacterial smear on a glass slide was air-dried and heat fixed. The sample was flooded with malachite green (Millipore Sigma, St. Louis, MO, USA) and steamed for 5 min. After rinsing with distilled water, the sample was counterstained with safranin (Millipore

Sigma, St. Louis, MO, USA) for 30 s, rinsed, and heat-fixed before being observed under a 100× objective.

2.4.2. Production of Pellicles

JunSE1L cells were initially pre-grown in a liquid minimal medium. Following the pre-growth phase, the cells were washed twice with distilled water to remove any residual medium. Subsequently, 100 µL of the washed cell suspension was transferred into separate flasks containing 100 mL of either minimal medium or LB medium. The cultures were incubated on a bench top at 22 °C without shaking. To monitor the growth and behavior of the cells, pictures were taken at regular time intervals throughout the incubation period.

2.4.3. Determination of Hemolysis Activity

The hemolysis activity of isolates was determined by noting zones of clearing around the colonies formed after bacteria were inoculated onto agar plates containing 5% sheep blood (Columbia blood agar, Hardy Diagnostics, Santa Maria, CA, USA). The JunSE1L cells were grown in LB at 22 °C with shaking at 140 rpm to mid-logarithmic phase before being washed in sterile water. Suspensions of the JunSE1L cells in sterile distilled water were applied in 10 µL aliquots (OD_{600} of 0.5) in triplicate to the blood agar plate. Growth was recorded at 30 °C. The assay was performed using three independent plates, each containing three colonies, representing technical replicates conducted within a single experiment.

2.4.4. Extracellular Protease Activity

Secretion of extracellular protease by JunSE1L was examined by observing zones of clearing around bacterial colonies growing on plates of Skim Milk Agar (SMA) medium (Medallion Milk Co., Winnipeg, MB, Canada) at 30 °C [38]. The assay was performed using three independent plates, each containing three colonies, representing technical replicates conducted within a single experiment.

2.4.5. Assessment of Phosphate Solubilization and Nitrogen Fixation

JunSE1L was grown by inoculating 100 µL of stock culture into 50 mL of minimal medium and incubating at 22 °C with shaking at 140 rpm for 48 h. The culture optical density (OD_{600}) was adjusted to 0.5. Cells were harvested by centrifugation at 16,000× *g* for 10 min, washed twice with sterile distilled water, and resuspended in distilled water.

Aliquots (20 µL) of the washed cell suspension were spotted onto Pikovskaya agar (HiMedia, Mumbai, India) to assess phosphate solubilization and onto Norris glucose nitrogen-free medium (2% agar; HiMedia, Mumbai, India) to evaluate nitrogen-fixing ability. Plates were incubated at 22 °C and monitored for colony growth and the formation of clearance zones around colonies. The assay was performed using three independent plates, each containing three colonies, representing technical replicates conducted within a single experiment.

2.4.6. Production of Surfactants

Surfactant production by JunSE1L was assessed over time during growth in a minimal medium (MM) broth. The minimal medium [39] contained buffered potassium phosphate (pH 7) (MP Biomedicals, Cat. No. 151946; Solon, OH, USA, Fisher Chemicals, Cat. No. P285; Fisher Scientific, Fair Lawn, NJ, USA), citrate (Mallinckrodt Chemicals, Cat. No. 0754-12; Phillipsburg, NJ, USA), and sucrose (Mallinckrodt AR, Cat. No. 8360; Paris, KY, USA) as carbon sources, and ammonium sulfate (Fisher Chemicals, Cat. No. A702; Fisher Scientific, Fair Lawn, NJ, USA) and magnesium sulfate (Fisher Scientific, Cat. No. M63; Fisher Scientific, Fair Lawn, NJ, USA) as the primary nitrogen, magnesium, and sulfur sources. Cultures were grown with shaking at 140 rpm at 22 °C. At defined time intervals between

14 and 48 h, growth was examined by measuring the OD_{600} nm of three samples of the culture. At the same time, three 1 mL aliquots were aseptically removed and centrifuged at 10,000× g for 10 min. The pelleted cells were discarded and the supernatant was filtered through a 0.22 µm filter. The surface tension of the filtrate was measured using a tensiometer (a wire probe tensiometer from Kibron Instruments, Malminkaari, Helsinki, Finland). Measurements were performed on three independent samples at each time point, and results are reported as mean ± standard deviation (SD). As controls for each sample, the surface tension of double-distilled sterile water and of absolute ethanol was measured. The temperature for these assays was 22 °C.

Partial purification of the surfactants involved precipitation at pH 2 followed by solubilization at pH 7 [40]. Culture filtrates of JunSE1L on MM grown for 3 d were adjusted to pH 2 by the addition of concentrated hydrochloric acid. After 14 h, the mixture was centrifuged at 10,000× g for 30 min, and the supernatant was removed by decantation. 5 mL of distilled water and 5 mL of 0.2 M NaOH were added to the pellet to bring the mixture to pH 7. After vortexing for 2 min, the solution was frozen at −80 °C for 16 h and lyophilized over 24 h. The mass of the flaky white product was used as the partially purified surfactant. The critical micelle concentration (CMC) of the isolated biosurfactant was determined from serial dilutions of a stock of 10 mg/mL of the pH 2-precipitated material. Subsequently, the surface tension of each dilution was measured using the tensiometer. Each dilution was measured in triplicate, and surface tension values are reported as mean ± SD. The CMC was determined as the concentration beyond which no further decrease in surface tension was observed.

2.4.7. Molecular Identification of the Seed Endophyte JunSE1L

To identify the endophyte, JunSE1L, a sample was incubated on a streaked plate of the bacteria for two days and a single colony was isolated in 1 mL of autoclaved distilled water, then boiled for 5 min, lysing the cells and releasing DNA. Once boiled and centrifuged to collect supernatant, the DNA was subjected to PCR. The PCR recipe was taken directly from the Master mix's protocol, GoTaq Green (Promega Corporation, Madison, WI, USA) and combined with primers centered on the 16S rRNA region of the bacterial genome. Specifically, 27F16S (5′ AGAGTTTGATCMTGGCTCAG 3′) and 1492R (5′ CGGTTACCTTGTTACGACTT 3′) [41] were used in combination with the extracted bacterial DNA and GoTaq Green master mix. A Techne Prime Thermocycler (Techne, Staffordshire, UK) was used with protocol obtained from GoTaq Green: initial denaturation at 95 °C for 5 min, then 35 cycles of denaturation at 95 °C for 30 s, annealing at 52 °C for 1 min, and extension at 72 °C for 1 min, with a final extension at 72 °C for 10 min. Once the PCR product was retrieved, gel electrophoresis was performed to ensure a single, strong band persisted in the product. The gel matrix consisted of agarose and Tris-Borate-EDTA (TBE) buffer with ethidium bromide as a fluorescent dye, electrophoresed at 100 V. After about 45 min, the gel was imaged using a GelDoc Go scanner (Bio-Rad Laboratories, Hercules, CA, USA) with UV light. After ensuring proper DNA isolation, a Monarch Spin PCR and DNA Cleanup Kit (New England Biolabs, Ipswich, MA, USA) was used to clean and prepare the PCR product for sequencing according to the manufacturer's protocol. 12 µL of the supplied elution buffer was used to elute the DNA. Analysis for purity and concentration was done on a NanoDrop One (Thermo Fisher Scientific, Waltham, MA, USA). The purified DNA was sent to Eton Bioscience (San Diego, CA, USA) for Sanger sequencing, and the sequence was identified using Basic Local Alignment Search Tool for nucleotides (BLASTN; NCBI, Bethesda, MD, USA), aligning against the NCBI nucleotide database. The sequence has been submitted to the NCBI GenBank database under accession PZ178898.

2.4.8. Molecular Confirmation of JunSE1L Identity in Recovered Plant-Associated Isolates

Representative colonies recovered from root tissues, shoot tissues, root wash suspensions, and sand wash samples were purified by three successive streaks on LB agar. A single colony from each isolate was suspended in sterile distilled water, and genomic DNA was extracted using a boiling lysis method as described above. The 16S rRNA gene was amplified using universal primers 27F (5′-AGAGTTTGATCMTGGCTCAG-3′) and 1492R (5′-CGGTTACCTTGTTACGACTT-3′) under the same PCR conditions described in Section 2.4.7. PCR products were verified by agarose gel electrophoresis, purified using a Monarch Spin PCR and DNA Cleanup Kit (New England Biolabs, Ipswich, MA, USA), and quantified using a NanoDrop One spectrophotometer (Thermo Fisher Scientific, Waltham, MA, USA). Purified amplicons were submitted to Eton Bioscience for Sanger sequencing. Resulting sequences were analyzed using NCBI BLASTn against the nucleotide database. A total of seven independent isolates ($n = 7$) from different plant compartments and associated samples were analyzed. Pairwise sequence alignment between recovered isolates and the JunSE1L reference sequence was additionally performed using the NCBI BLASTn "Align Two Sequences" tool, confirming 100% sequence identity.

2.5. Antifungal Activity of JunSE1L

2.5.1. Fungal Isolates and Molecular Identification

Fusarium proliferatum, a known pathogen of winter wheat, was obtained from the Utah Plant Pest Diagnostic Laboratory after isolation from a marble onion collected in Corrine, Utah. Another fungal isolate was included to assess broad-spectrum antifungal activity: recovered from infected turfgrass in Salt Lake County, Utah, provided by the Utah Plant Pest Diagnostic Laboratory.

For molecular identification of the turfgrass-associated fungi, each isolate was grown on solid medium for 48 h. Mycelial material was collected using a sterile loop and transferred to 1.5 mL microcentrifuge tubes for DNA extraction. Genomic DNA was isolated using the DNeasy Plant Mini Kit (QIAGEN, Hilden, Germany) following the manufacturer's protocol, with elution volumes reduced to 50 µL (two elutions).

The internal transcribed spacer (ITS) region was amplified using primers ITS5 (5′-GGAAGTAAAAGTCGTAACAAGG-3′) and ITS4 (5′-TCCTCCGCTTATTGATATGC-3′) with repliQa HiFi ToughMix (Quantabio, Beverly, MA, USA). PCR cycling conditions consisted of 40 cycles of 95 °C for 10 s, 52 °C for 5 s, and 68 °C for 1 s. Amplicons were verified by agarose gel electrophoresis in TBE buffer containing ethidium bromide to visualize DNA and then purified using the Monarch PCR & DNA Cleanup Kit (New England Biolabs). Purified products were sequenced by Sanger sequencing (Eton Bioscience), and sequences were identified using BLAST (https://blast.ncbi.nlm.nih.gov/Blast.cgi, accessed on 23 May 2026) against the NCBI nucleotide database.

2.5.2. Antifungal Activity Assay

Frozen stocks of JunSE1L (15% glycerol) were revived in 50 mL LB and incubated at 22 °C with shaking (140 rpm). Cultures were subcultured once into fresh LB and grown for 24 h. Cells were harvested and adjusted to $OD_{600} = 0.5$ using fresh LB. The culture was centrifuged at 16,000× *g* for 10 min, and the pellet was washed once and resuspended in sterile distilled water for use in antifungal assays.

Fungal inocula were prepared by suspending actively growing mycelial material in sterile distilled water and vortexing to obtain a uniform suspension. Aliquots (100 µL) of the fungal suspension were spread evenly onto LB agar plates (2% agar) and allowed to dry under sterile conditions.

A 10 µL drop of the OD-adjusted JunSE1L suspension was placed at the center of each fungal plate. Control plates received a 10 µL drop of sterile distilled water applied to the agar surface. Plates were incubated at 22 °C for 4 days and examined for zones of reduced fungal growth surrounding the bacterial inoculation site. Zone of inhibition (ZOI) diameters were quantified using ImageJ software (version 1.54g; National Institutes of Health, Bethesda, MD, USA) by measuring four diameters per inhibition zone and averaging to obtain a single value per replicate. Three technical replicates were analyzed for each condition, and results are reported as mean ± SD.

2.5.3. Antifungal Activity of Cell-Free Culture Supernatant

To assess the contribution of extracellular metabolites, JunSE1L was grown in LB for 48 h under the conditions described above. Cultures were centrifuged twice at 4000× *g* for 20 min to remove cells, and the supernatant was filtered through a 0.22 µm membrane to obtain sterile cell-free culture supernatant. Sterility of the filtrate was confirmed by plating an aliquot onto LB agar.

Sterile 6 mm Grade 1 Whatman filter paper disks were immersed in the supernatant for 15 s and placed onto fungal lawns prepared as described above. Control disks were soaked in sterile distilled water for the same duration. Plates were incubated at 22 °C for 4 days and examined for inhibition zones surrounding the disks.

2.6. Seed Surface Inoculation Assay

Surface-sterilized wheat seeds (as described above) were inoculated with JunSE1L to evaluate its potential for seed biopriming. JunSE1L was grown in MM at 22 °C to mid-log phase ($OD_{600} \approx 0.75$). Cells were harvested by centrifugation at 16,000× *g* for 10 min, washed twice with sterile distilled water, and resuspended to the desired concentrations. Bacterial suspensions were prepared in sterile distilled water across a range of concentrations (10^4–10^8 CFU mL^{-1}), with cell densities estimated by OD–CFU calibration and confirmed by direct plating on 2% LB agar.

Individual seeds were placed in sterile 1.5 mL microcentrifuge tubes containing 1 mL of the respective bacterial suspension (one seed per tube). Tubes were capped and incubated under static conditions at 22 °C to allow surface attachment. For the lowest concentration (10^4 CFU mL^{-1}), incubation times of 10 and 30 min were tested, while all other concentrations (10^5–10^8 CFU mL^{-1}) were incubated for 10 min to assess concentration-dependent attachment.

Experiments at 10^4 and 10^8 CFU mL^{-1} were performed using three independent biological replicates, each with three technical replicates, whereas intermediate concentrations (10^5–10^7 CFU mL^{-1}) were evaluated using three technical replicates.

Following inoculation, individual seeds were removed using sterile tweezers and gently shaken to remove excess liquid. Residual droplets were further removed by briefly dabbing seeds on sterile Kimwipes™.

To quantify bacterial attachment, each seed was transferred into 1 mL sterile distilled water and vortexed for 30 s to detach surface-associated cells. Serial 10-fold dilutions were prepared, and 100 µL aliquots were plated onto 2% LB agar. Plates were incubated at 22 °C for 72 h before colony enumeration. Colony-forming units (CFU) were calculated and normalized per seed.

3. Results

3.1. Isolation of Juniper Wheat Seed Endophyte JunSE1L

White bacterial colonies emerged from approximately 80% (44 out of 55 seeds) of surface-sterilized seeds of the wheat cultivar Juniper when germinated on LB 2% agar

(Figure 1A). Colony development was visually similar among most seeds and consisted of opaque white colonies with raised edges forming in close proximity to the seed. Bacterial growth was consistently observed surrounding the germinating seeds but was not detected when intact root or shoot tissues contacted the LB agar surface during early seedling development. Because these colonies arose from surface-sterilized seeds under sterile conditions, they were considered seed-associated endophytes.

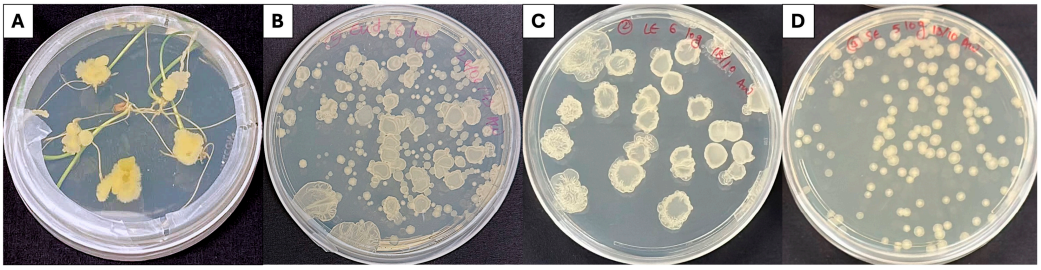

Figure 1. Isolation and colony morphology of bacteria emerging from surface-sterilized wheat seeds (cv. Juniper). (**A**) White bacterial colonies emerging from germinating wheat seeds with an emergence rate of 80% (44 out of 55 seeds) after 4 days of incubation on LB agar. (**B**) Colony morphology observed after dilution plating of bacteria recovered from a single seed shown in (**A**), revealing two distinct colony sizes. (**C**) Large, rugose colonies of the isolate designated JunSE1L after 4 days of growth on LB agar. (**D**) Smaller, smooth colonies of the isolate designated JunSE1S after 4 days of growth on LB agar.

Purification by streaking to single colonies on LB agar yielded two distinct colony morphologies. One morphology produced large, rugose colonies, while the second consisted of smaller, smoother colonies (Figure 1B). The large-colony isolate was designated JunSE1L (Figure 1C), and the smaller colony variant was termed JunSE1S (Figure 1D). These designations are based on colony morphology and do not imply taxonomic distinction. Both colony morphologies were stable and retained through repeated transfers on LB agar. Subsequent characterization in this study focused on the JunSE1L isolate.

3.2. Seed-Origin Endophyte Detected in Multiple Plant Compartments from Seedlings Grown in Sterile Sand

Colonies morphologically similar to JunSE1L were recovered from several plant-associated niches after six days of growth of surface-sterilized seeds in sterile sand in closed Magenta™ boxes. Bacteria were detected in the rhizosphere from sand adhering to the roots (Figure 2A). In rhizoplane assays, colony formation was observed from root wash suspensions and from plated root segments (Figure 2B,C), indicating the presence of bacteria associated with root surfaces or closely associated root tissues.

Colonies with morphology consistent with JunSE1L were also recovered from aerial plant tissues. Growth developed from leaf and shoot segments placed on LB agar after harvest (Figure 2D). Bacterial emergence was most frequently observed from cut edges of roots and shoots rather than from intact tissues. Colonies were rarely detected when intact plant surfaces were placed directly on agar.

Some variation in colony appearance compared with colonies emerging directly from germinating seeds (Figure 1A) was observed. This difference likely reflects variation in local moisture availability and surface drying of LB agar during incubation, conditions known to influence colony spreading, matrix production, and colony architecture in *Bacillus* biofilms [42,43].

To further confirm the internal origin of the endophyte, surface-sterilized seeds were also germinated directly on 2% LB agar plates without transfer to sand systems. After five days of growth, roots and shoots were aseptically cut using sterile tweezers. A JunSE1L-

like endophyte consistently emerged from the cut ends of both roots and shoots, and its temporal emergence is documented in Figures S1 and S2.

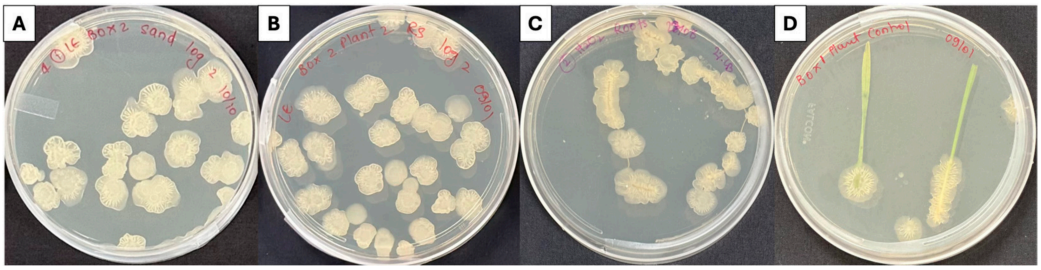

Figure 2. Recovery of JunSE1L-like colonies from harvested wheat tissues. (**A**) Bacterial colonies recovered from rhizosphere sand adhering to roots of seedlings grown from surface-sterilized seeds. (**B**) Colonies obtained from root wash suspensions indicating rhizoplane-associated bacteria. (**C**) Colony development from plated root segments following harvest. (**D**) Colonies emerging from leaf and shoot tissues placed on LB agar. In most cases, bacterial growth was observed from cut edges of plant tissues rather than intact surfaces. Colonies recovered from plant tissues displayed morphology consistent with the JunSE1L isolate when grown on LB medium. Experiments were conducted under sterile conditions as described in Methods.

To verify the identity of colonies recovered from plant tissues and associated samples, representative isolates from roots, shoots, root wash suspensions, and sand wash samples were purified and subjected to 16S rRNA gene sequencing. Sequence analysis using NCBI BLASTn showed that all isolates analyzed (n = 7) exhibited 100% identity to the JunSE1L isolate, which was identified as *Bacillus atrophaeus* by 16S rRNA gene sequencing as described in Section 3.7, confirming that the recovered colonies correspond to the original seed-associated endophyte.

Together, the consistent recovery of morphologically similar colonies across multiple plant compartments, combined with molecular confirmation of representative isolates, supports the persistence and dissemination of the seed-associated endophyte during early seedling development.

3.3. Nutrient-Dependent Growth Plasticity of JunSE1L

JunSE1L displayed pronounced differences in colony morphology and development depending on nutrient conditions (Table 1). On LB agar (2% agar), colonies remained compact and wrinkled with limited lateral spreading. Colony diameter ranged from 1.1 $\pm$ 0.1 cm at day 3 to 1.5 $\pm$ 0.1 cm by day 7. In contrast, colonies grown on MM spread widely and exhibited a flatter morphology, reaching 2.4 $\pm$ 0.2 cm by day 3 and expanding to 4.1 $\pm$ 0.6 cm by day 5.

Colony surface wetting behavior, used here as a qualitative indicator of surface hydrophobicity, also differed between growth conditions. Water droplets applied to LB-grown colonies remained spherical for approximately 1.5–2 h, suggesting a more hydrophobic colony surface phenotype under these conditions. This phenotype appeared by day 3 and persisted through day 15. In contrast, droplets placed on MM-grown colonies flattened rapidly and were absorbed into the colony surface within approximately 10 min, suggesting a less hydrophobic or more wettable colony surface phenotype. Because contact angle measurements were not performed, these observations were interpreted qualitatively rather than quantitative measurements of hydrophobicity.

Sporulation timing also differed between the two media. In MM-grown colonies, spores within mother cells were first observed by day 5, and free spores were detected by day 7. In contrast, sporulation was delayed in LB-grown colonies, where spores within

mother cells were first detected only after 15 days of incubation. Sporulation was assessed qualitatively by microscopic observation of malachite green-stained cells.

Table 1. Nutrient-dependent changes in colony growth, qualitative surface wetting/hydrophobicity phenotype, and sporulation of JunSE1L on LB and minimal media.

Day	Qualitative Hydrophobicity Phenotype		Spore Formation		Colony Diameter (cm) (2% Agar)	
	LB	MM	LB	MM	LB	MM
3	+	-	-	-	1.1 ± 0.1	2.4 ± 0.2
5	+	+/−	-	Within the mother cell	1.1 ± 0.0	4.1 ± 0.6
7	+	+/−	-	Free	1.5 ± 0.1	4.0 ± 0.5
9	+	+/−	-	Free	N/A	N/A
15	+	+/−	Within the mother cell	Free	N/A	N/A

Qualitative hydrophobicity phenotype was assessed by observing sterile water droplet behavior on colony surfaces. A "+" indicates formation of a stable, nearly spherical droplet, while "+/–" indicates droplet flattening followed by absorption into the colony surface within approximately 10 min. Contact angle measurements were not performed; therefore, these scores represent observational surface-wetting phenotypes rather than quantitative hydrophobicity measurements. Spore formation was detected using malachite green staining and categorized as spores within mother cells or free spores following release. Colony diameter represents the maximum colony dimension measured for colonies grown on agar surfaces.

Together, these observations demonstrate strong nutrient-dependent developmental plasticity in JunSE1L, affecting colony architecture, qualitative surface wetting behavior, and sporulation dynamics.

3.4. Surface-Associated Growth and Biofilm Formation

Additional phenotypes supported a surface-associated lifestyle for JunSE1L. Colonies grown on LB developed a rugose morphology and strong colony surface hydrophobicity (Figure 3B), consistent with the production of surface-active or hydrophobic cell envelope components. In static liquid cultures, JunSE1L formed a thick pellicle at the air-liquid interface in LB within 48 h (Figure 3D), indicating robust biofilm formation.

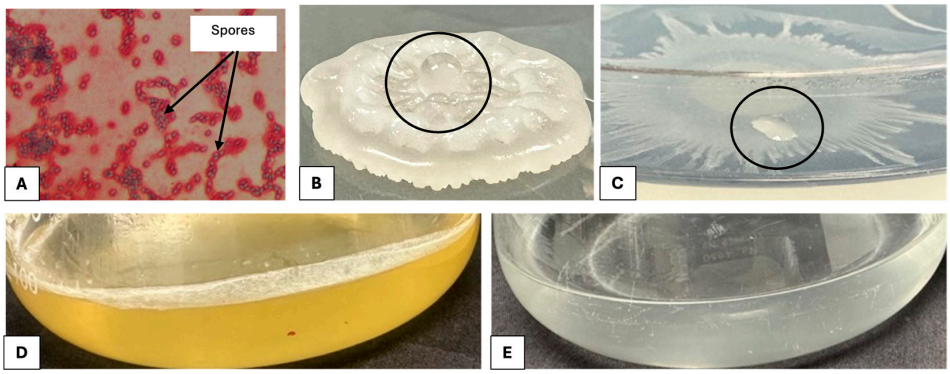

Figure 3. Surface-associated traits and biofilm formation in JunSE1L. (**A**) Spore production by JunSE1L after 15 days of incubation on LB agar (2% agar). Spores are stained green with malachite green (arrows), while vegetative cells are counterstained pink with safranin. (**B**) Hydrophobic colony surface after 3 days of growth on LB agar, demonstrated by retention of a nearly spherical water droplet for at least 2 h. The circle highlights the water droplet. (**C**) Colony surface on MM agar after 7 days, where the water droplet flattened and was absorbed within 10 min, indicating reduced hydrophobicity. The circle highlights the water droplet. (**D**) Pellicle formation by JunSE1L after 48 h incubation in static LB medium, showing a thick biofilm at the air-liquid interface. (**E**) Absence of pellicle formation in minimal medium under identical static conditions.

In contrast, no visible pellicle or appreciable surface biomass developed in minimal medium under the same static conditions (Figure 3E), suggesting that biofilm formation in JunSE1L is enhanced under nutrient-rich conditions.

3.5. Extracellular Lytic Activities and Nutrient-Mobilization Traits

JunSE1L exhibited extracellular lytic activities when grown on diagnostic media. Colonies produced clear hemolytic zones on blood agar after 3 days of incubation, indicating hemolytic activity (Figure 4A). Growth on skim milk agar also resulted in zones of casein hydrolysis surrounding colonies, demonstrating secretion of extracellular proteases (Figure 4B).

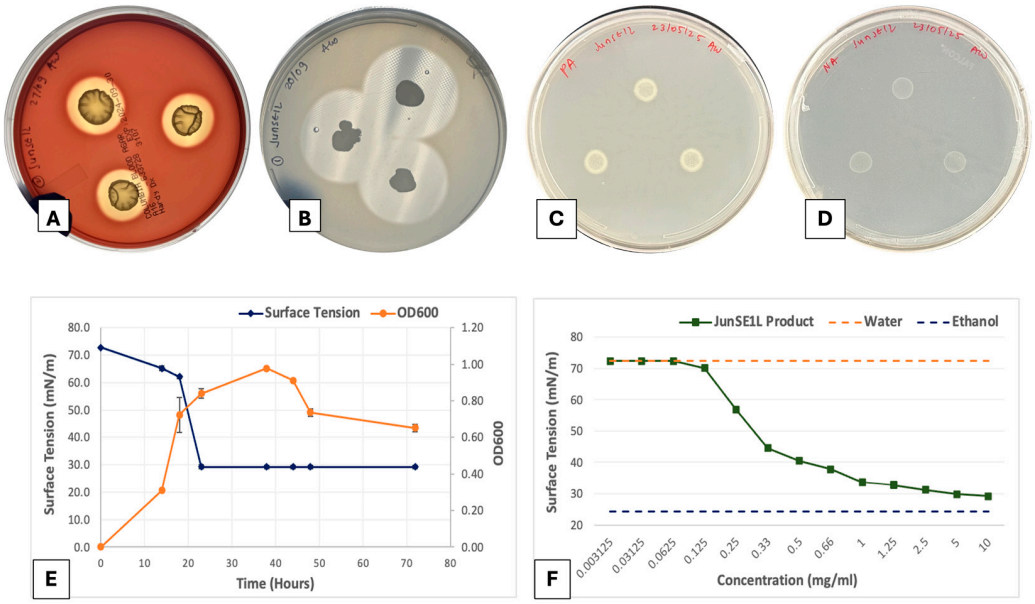

Figure 4. Extracellular lytic activities, nutrient-mobilization traits, and biosurfactant production by JunSE1L. (**A**) Hemolytic activity of JunSE1L on blood agar after 3 days of incubation, indicated by zones of clearing surrounding colonies. (**B**) Proteolytic activity on skim milk agar showing casein hydrolysis surrounding colonies after 3 days of growth. (**C**) Growth of JunSE1L on Pikovskaya agar showing no detectable phosphate-solubilizing activity under the conditions tested. (**D**) Growth of JunSE1L on nitrogen-free medium indicating absence of detectable nitrogen-fixing capability. (**E**) Relationship between bacterial growth (OD_{600}) and reduction in surface tension of culture supernatant during growth of JunSE1L in liquid minimal medium. Surface tension decreased from that of pure water to approximately 30 mN m^{-1} during late exponential growth. (**F**) Relationship between surface tension and concentration of the pH-2-precipitated biosurfactant fraction used to estimate the CMC. Error bars represent three biological replicates; values fall within the symbols.

In contrast, no zones of clearance were observed on Pikovskaya agar, indicating the absence of detectable phosphate-solubilizing activity under the conditions tested (Figure 4C). Similarly, growth on nitrogen-free medium did not indicate nitrogen-fixing capability (Figure 4D). Together, these observations suggest that JunSE1L lacks classical nutrient-mobilization traits but produces extracellular lytic activities commonly associated with microbial competition.

3.6. Production of Extracellular Biosurfactant

Growth of JunSE1L in liquid minimal medium resulted in a growth-phase-dependent reduction in surface tension of the culture filtrate. Surface tension decreased from 72.2 mN m^{-1} (pure water) to approximately 30 ± 0.01 mN m^{-1} (mean ± SD, n = 3) by 38 h of growth (Figure 4E). The decline began at approximately 34 h and corresponded

to the late exponential growth phase, during which cell density increased from an initial ~10^6 CFU mL^{-1} to 5 ($\pm$1) $\times$ 10^8 CFU mL^{-1}.

Surface-active compounds were recovered from cell-free culture supernatant by acid precipitation at pH 2 and retained activity after resuspension at neutral pH. Surface tension measurements of serial dilutions of the isolated material were used to estimate the CMC, which was approximately 0.125 mg mL^{-1} (Figure 4F). The gradual transition in surface tension across an order of magnitude of extract concentration suggests that multiple surface-active molecules may contribute to the observed reduction in surface tension.

3.7. Molecular Identification of the Seed Endophyte JunSE1L

Phenotypic characteristics of JunSE1L—including colony morphology, sporulation, biosurfactant production, hemolytic activity, and extracellular protease secretion—suggested affiliation with the genus *Bacillus*. PCR amplification of the 16S rRNA gene followed by sequencing and BLAST analysis identified the isolate as *Bacillus atrophaeus* with 100% sequence identity. These results confirm that the seed-derived endophyte JunSE1L belongs to the species *Bacillus atrophaeus*.

3.8. Identification of Fungal Isolates Used in Antifungal Assays

The turfgrass-associated fungal isolate used in antifungal assays was identified as *Mucor hiemalis* based on ITS region sequencing and BLAST analysis (100% sequence identity). The *Fusarium proliferatum* isolate used in this study had been previously identified by the Utah Plant Pest Diagnostic Laboratory using the same approach.

3.9. Antifungal Activity of JunSE1L

JunSE1L inhibited fungal growth when applied as a live bacterial suspension. When a 10 µL drop of the 0.5 OD_{600} bacterial suspension was placed at the center of plates inoculated with fungal lawns, clear zones of reduced fungal growth developed surrounding the bacterial inoculation site after 4 days of incubation at 22 °C. Quantitative analysis of inhibition zones revealed that JunSE1L produced a ZOI of 3.0 $\pm$ 0.2 cm for *Mucor hiemalis* and 2.0 $\pm$ 0.0 cm for *Fusarium proliferatum* (mean $\pm$ SD, n = 3) (Figure 5A,B), indicating antagonistic activity against both fungi. The antifungal assay was designed to determine whether detectable inhibition occurred under each assay condition, rather than to statistically compare relative sensitivity between fungal species; therefore, ZOI values are reported descriptively as mean $\pm$ SD.

To determine whether cell-free extracellular activity contributed to this effect, sterile filter paper disks were dipped in cell-free culture supernatant of JunSE1L for approximately 15 s and then placed onto fungal lawns. Under these conditions, inhibition zones were observed around disks containing the JunSE1L supernatant for *Mucor hiemalis*, with a ZOI of 1.5 $\pm$ 0.2 cm (mean $\pm$ SD, n = 3), showing that the cell-free supernatant retained inhibitory activity against this fungus under the tested conditions. In contrast, no detectable inhibition (0 cm) was observed against *Fusarium proliferatum* when treated with the same supernatant (Figure 5C,D).

The different responses observed between live-cell and cell-free supernatant assays indicate that antifungal activity was influenced by both assay format and fungal species. While *F. proliferatum* was inhibited in the presence of live JunSE1L cells, the tested cell-free supernatant did not produce a comparable inhibitory effect. The mechanism underlying this difference was not determined in the present study. Therefore, these results should be interpreted as assay- and species-dependent antifungal activity under the tested conditions, rather than as evidence of strict target specificity or a defined enzymatic or metabolite-mediated mechanism.

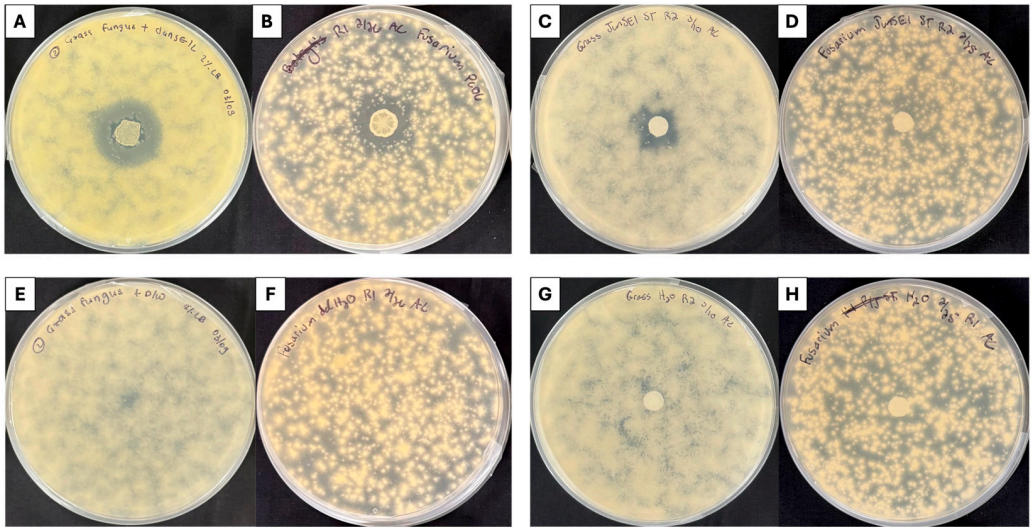

Figure 5. Antifungal activity of JunSE1L against *Mucor hiemalis* and *Fusarium proliferatum*. (**A**,**B**) Inhibition of fungal growth by live JunSE1L cells. A 10 µL drop of OD_{600}-adjusted bacterial suspension was placed at the center of fungal lawns and incubated for 4 days at 22 °C. (**A**) *M. hiemalis*; (**B**) *F. proliferatum*. (**C**,**D**) Inhibition by cell-free culture supernatant applied using sterile filter paper disks. (**C**) *M. hiemalis*; (**D**) *F. proliferatum*. (**E**,**F**) Control treatments using sterile distilled water applied directly to the agar surface. (**E**) *M. hiemalis*; (**F**) *F. proliferatum*. (**G**,**H**) Control treatments using sterile filter paper disks dipped in sterile distilled water. (**G**) *M. hiemalis*; (**H**) *F. proliferatum*. No inhibition was observed in control treatments.

Control treatments using sterile distilled water showed no inhibition of fungal growth. For disk controls, sterile filter paper disks were dipped in sterile distilled water for approximately 15 s before being placed on the agar surface, while additional controls received sterile distilled water applied directly to the agar surface (Figure 5E–H).

Together, these results demonstrate that JunSE1L exhibits antifungal activity against both fungi in live-cell assays, while cell-free supernatant activity was detected against *M. hiemalis* but not *F. proliferatum* under the tested conditions. The biochemical basis for this differential response remains unresolved and requires further investigation.

3.10. Inoculum-Density-Dependent Recovery of JunSE1L from Wheat Seed Surfaces

To assess whether JunSE1L could be applied as a seed inoculant for biopriming applications, surface inoculation experiments were performed across a range of bacterial concentrations. At 10^4 and 10^5 CFU mL^{-1}, minimal to no bacterial attachment was detected on the seed surface following incubation, even after extended exposure times (Figure S3). In contrast, inoculation at 10^8 CFU mL^{-1} resulted in ~10^5 CFU per seed recovery, indicating successful attachment at higher cell densities.

Experiments with intermediate concentrations (10^5–10^7 CFU mL^{-1}) further demonstrated a concentration-dependent increase in bacterial attachment. Notably, inoculation at 10^6 CFU mL^{-1} resulted in ~10^2 CFU per seed recovery, confirming that attachment is not absent at lower concentrations but scales with inoculum density.

Radicle emergence was observed across all tested JunSE1L inoculum densities, including the highest concentration tested. At 10^8 CFU mL^{-1}, seeds showed visible radicle emergence and were classified as germinated; however, early seedling growth varied among individual seeds. Because root length, shoot height, and dry biomass were not quantitatively measured, seedling vigor was not assessed from these observations. Thus, the results support an inoculum-density-dependent increase in JunSE1L recovery

from the seed surface, while the effect of high-density inoculation on early seedling vigor remains unresolved.

Overall, higher starting inoculum densities improved recovery of JunSE1L from wheat seed surfaces under the tested conditions. Additional controlled experiments measuring germination percentage, root length, shoot height, and biomass will be needed to determine whether increased seed surface recovery influences early seedling performance or host compatibility.

4. Discussion

16S rRNA analysis identified the wheat-associated isolate JunSE1L as *Bacillus atrophaeus*, and physiological characterization revealed traits consistent with a stress-tolerant, surface-associated plant colonizer with antifungal potential. Members of the *Bacillus* genus are widely recognized for their ecological versatility, persistence through sporulation, and ability to suppress plant pathogens through biofilm formation and secretion of antimicrobial metabolites [44]. The functional profile observed for JunSE1L aligns with these characteristics and suggests that, under the conditions tested, its plant-associated role may be more closely linked to persistence and biocontrol-related activity than to direct nutritional plant-growth promotion.

The colony and pellicle phenotypes suggest that JunSE1L readily adopts a surface-associated lifestyle, with nutrient availability shaping whether the population remains in a biofilm state or shifts toward dormancy. In *Bacillus*, these transitions are governed by interconnected regulatory pathways that couple matrix production, multicellular behavior, and entry into sporulation [45–47]. The low surface tension of the culture supernatant is also consistent with lipopeptide biosurfactant production, which in *Bacillus* promotes surface spreading and accelerates pellicle development, while hydrophobin-like matrix components such as BslA can generate the hydrophobic barrier characteristic of mature biofilms [22,48–51]. Together, these traits support the idea that JunSE1L is well adapted to persist on exposed plant surfaces where fluctuating moisture, nutrient supply, and competition favor organized multicellular growth.

Consistent with this surface-associated phenotype, JunSE1L also exhibited antifungal activity under laboratory assay conditions. JunSE1L cell-free supernatant retained inhibitory activity against *M. hiemalis* under the tested conditions. However, the lack of detectable inhibition of *F. proliferatum* by the cell-free supernatant should be interpreted cautiously. Because *F. proliferatum* was inhibited by live JunSE1L cells but not by the supernatant disk assay, this difference indicates that antifungal activity differed between live-cell and cell-free assay formats. Therefore, these results are best interpreted as differences in antifungal activity under the tested assay conditions rather than evidence of strict fungal target specificity. This interpretation is consistent with previous reports showing that antifungal metabolites produced by *Bacillus* spp., including lipopeptides such as iturins, fengycins, and surfactins, can vary in activity depending on fungal species, exposure conditions, and local concentration [35,52]. In structured growth environments, secreted metabolites may also accumulate near bacterial colonies or within biofilm-associated matrices, potentially increasing their local activity compared with cell-free supernatant assays [43,53].

From an ecological perspective, the antifungal activity of JunSE1L may be relevant to early plant-associated microbial interactions, where seed- and root-associated bacteria encounter diverse fungal taxa in the surrounding environment. In this study, *M. hiemalis* and *F. proliferatum* showed different responses to live JunSE1L cells and to cell-free supernatant, indicating that antifungal activity was influenced by both the fungal target and the assay format. The inhibition of *M. hiemalis* by the cell-free supernatant demonstrates that inhibitory activity was present in the cell-free fraction under the tested conditions.

In contrast, the lack of detectable supernatant-mediated inhibition against *F. proliferatum* indicates that this activity was not equally effective across both fungi in the disk assay. Therefore, these results should be interpreted as evidence of assay- and fungus-dependent antifungal activity, rather than as direct evidence of ecological specificity. Together, the findings suggest that JunSE1L has the capacity to inhibit fungal growth through live-cell-associated activity and, in some cases, through cell-free extracellular activity, although the outcome depends on the fungal species and experimental conditions. Future work using compound identification, enzyme-inactivation assays, and purified fractions would be needed to determine the mechanism responsible for the observed antifungal activity.

An additional finding from this study is that JunSE1L recovery varied depending on plant compartment and growth stage. Although JunSE1L was not recovered from intact root or shoot tissues during early seed germination, colonies recovered at later sampling points from the rhizosphere, rhizoplane, and aerial plant compartments were confirmed as JunSE1L by 16S rRNA gene sequencing, showing 100% sequence similarity to the original JunSE1L isolate. These results indicate that JunSE1L can be recovered from multiple wheat-associated compartments over time, although further work using strain-specific tracking would be needed to define its colonization dynamics and spatial localization more precisely. This pattern suggests that JunSE1L detection may depend on sampling time, plant compartment, and bacterial abundance during seedling development. This interpretation is consistent with previous studies showing that seed-associated microbes can contribute to early microbiome assembly and influence colonization of plant-associated compartments, including the rhizosphere and phyllosphere [54,55]. Responses of *B. atrophaeus* and related species to root exudates may further support plant-associated surface colonization behaviors under suitable conditions [56].

In the context of winter wheat, which undergoes vernalization and is exposed to prolonged low temperatures, the ability of JunSE1L to form spores may be relevant for persistence under stressful conditions. Sporulation is a well-known survival strategy that enables *Bacillus* cells to tolerate environmental stress. In this study, the recovery of JunSE1L from wheat-associated compartments over time suggests that this isolate can persist during early seedling development under the tested conditions. However, the role of sporulation in JunSE1L persistence during vernalization or cold exposure was not directly tested and should be evaluated in future work.

From an applied perspective, these observations are relevant for understanding the use of *Bacillus* species as seed-priming agents in agriculture. *Bacillus* strains are commonly applied as spores or powder-based formulations to enhance seed colonization, improve germination, and provide early protection against soil-borne pathogens [57,58]. However, in this study, surface inoculation of wheat seeds with vegetative cells of JunSE1L was inefficient at lower concentrations (10^4 and 10^5 CFU mL^{-1}) and required high cell densities (10^6–10^8 CFU mL^{-1}) to achieve detectable attachment. At the highest inoculum level tested, increased bacterial recovery was observed, and seeds showed visible germination based on radicle emergence. However, early seedling growth appeared variable among individual seeds, and root length, shoot height, and dry biomass were not quantitatively measured. Therefore, the present data do not support a statistically confirmed conclusion that high-density JunSE1L inoculation reduces seedling vigor.

Thus, under the tested conditions, vegetative-cell inoculation showed an inoculum-density-dependent effect on bacterial recovery from the seed surface, but its effect on seedling vigor remains unresolved. The novelty of JunSE1L lies in its recovery as a naturally seed-associated wheat endophyte with multiple bioactive traits, including motility, surface-associated growth, biosurfactant-related activity, and antifungal potential. These traits suggest that JunSE1L may be a useful model for studying how native seed-associated

Bacillus strains contribute to early plant microbiome assembly. From an application perspective, the concentration-dependent recovery observed here indicates that inoculation dose should be carefully optimized, since higher cell densities improved bacterial recovery but were associated with reduced early seedling performance. Further studies comparing vegetative cells, spores, and alternative delivery methods would be needed to determine the most effective approach for establishing JunSE1L on wheat seeds while maintaining normal germination and seedling vigor.

This perspective also helps explain the ecological function of JunSE1L during early plant development. As seedlings grow in soil, roots and shoots experience mechanical abrasion, micro-wounding, and interactions with soil microorganisms and microfauna. Such processes may release bacteria from protected internal seed-associated niches, allowing them to colonize newly exposed plant surfaces. Once established, these bacteria can occupy attachment sites, form biofilms, and interact directly with surrounding microbial communities. In this context, JunSE1L may function as a mobile defensive population originating from the seed endosphere and recruited to plant surfaces during early development, where it can contribute to microbial competition and pathogen suppression.

Beyond direct antagonism, some *Bacillus* species can influence plant defense responses through induced systemic resistance (ISR). Bacterial lipopeptides, including surfactin and fengycin, have been reported to act as microbe-associated molecular patterns (MAMPs) that activate plant defense signaling pathways and prime plants for responses to pathogen challenge [35,59]. However, ISR was not directly evaluated in the present study, and no conclusions can be drawn regarding host immune activation by JunSE1L. The present results show that JunSE1L can be recovered from multiple wheat-associated compartments over time and exhibits antifungal activity under the tested in vitro conditions. Future studies evaluating plant defense markers, pathogen challenge assays, and strain-specific colonization would be needed to determine whether JunSE1L also contributes to host defense responses in planta.

5. Conclusions

This study identified the wheat seed-derived endophyte JunSE1L as *Bacillus atrophaeus* and demonstrated that it exhibits multiple traits associated with plant-associated bacteria, including nutrient-dependent changes in colony architecture, biofilm formation, sporulation, and biosurfactant production. JunSE1L was recovered from rhizosphere, rhizoplane, and aerial plant compartments following seed germination. In antifungal assays, live JunSE1L cells inhibited both *Fusarium proliferatum* and *Mucor hiemalis*, whereas the cell-free supernatant inhibited *M. hiemalis* but not *F. proliferatum* under the tested conditions. These results indicate that antifungal activity depends on both fungal species and assay format and should not be interpreted as strict target specificity.

Overall, JunSE1L represents a wheat-associated endophyte with bioactive traits under laboratory conditions and the ability to recover from multiple plant-associated compartments over time. Seed surface inoculation with vegetative cells showed concentration-dependent recovery, with higher inoculum levels improving bacterial recovery from the seed surface. Further work is needed to evaluate whether alternative delivery methods can improve JunSE1L establishment while maintaining normal germination and seedling vigor.

Supplementary Materials: The following supporting information can be downloaded at https://www.mdpi.com/article/10.3390/seeds5030030/s1. Figure S1: Emergence of endophyte from cut shoot tissue; Figure S2: Emergence of endophyte from cut root tissue; Figure S3: Concentration-dependent attachment of JunSE1L to wheat seeds.

Author Contributions: Conceptualization, A.W. and D.B.; methodology, A.W. and D.B.; validation, A.W. and D.B.; formal analysis, A.W.; investigation, A.W., Z.X. and A.C.; resources, D.B.; data curation, A.W., Z.X. and A.C.; writing—original draft preparation, A.W.; writing—review and editing, A.W., A.C. and D.B.; visualization, A.W. and D.B.; supervision, D.B.; project administration, D.B.; funding acquisition, D.B. All authors have read and agreed to the published version of the manuscript.

Funding: This research was funded by USDA-NIFA Award 2024-67022-42830 and UAES Project UTAO-1581. The funding bodies had no role in the design of the study; collection, analysis, or interpretation of data; or in writing the manuscript.

Institutional Review Board Statement: Not applicable.

Informed Consent Statement: Not applicable.

Data Availability Statement: All data generated or analyzed during this study are included in this published article and its Supplementary Information Files. Additional datasets supporting the conclusions of this article are available from the corresponding author upon reasonable request.

Acknowledgments: The authors thank members of the Britt Lab for helpful discussions and technical assistance, including Kai Heftel for providing additional observations on the release of seed-associated bacteria into sand during wheat seedling growth. We are especially grateful to Anne Anderson for her constant support, insightful guidance, and fruitful scientific discussions throughout this study. We also thank Claudia Nischwitz from the Biology Department at Utah State University for providing fungal cultures for antifungal assays and for access to her laboratory facilities for DNA extraction of fungal isolates and the endophyte JunSE1L. We acknowledge institutional support from Utah State University. During the preparation of this manuscript, the authors used ChatGPT (GPT-5.5, OpenAI) to assist with language editing and drafting of text. The authors have reviewed and edited the output and take full responsibility for the content of this publication.

Conflicts of Interest: The authors declare no conflicts of interest. The funders had no role in the design of the study; in the collection, analyses, or interpretation of data; in the writing of the manuscript; or in the decision to publish the results.

Abbreviations

The following abbreviations are used in this manuscript:

ISR	Induced Systemic Resistance
H_2O_2	Hydrogen peroxide
LB	Lysogeny Broth
CFU	Colony Forming Units
SMA	Skim Milk Agar
OD	Optical Density
MM	Minimal Medium
RPM	Revolutions per minute
CMC	Critical Micelle Concentration
PCR	Polymerase Chain Reaction
UV	Ultraviolet
ZOI	Zone of Inhibition
SD	Standard Deviation
BLAST	Basic Local Alignment Search Tool
MAMPs	Microbe Associated Molecular Patterns

References

1. Truyens, S.; Weyens, N.; Cuypers, A.; Vangronsveld, J. Bacterial seed endophytes: Genera, vertical transmission and interaction with plants. *Environ. Microbiol. Rep.* **2015**, *7*, 40–50. [CrossRef]

2. Bokhari, A.; Essack, M.; Lafi, F.F.; Andres-Barrao, C.; Jalal, R.; Alamoudi, S.; Razali, R.; Alzubaidy, H.; Shah, K.H.; Siddique, S.; et al. Bioprospecting desert plant *Bacillus* endophytic strains for their potential to enhance plant stress tolerance. *Sci. Rep.* **2019**, *9*, 18154. [CrossRef]
3. Sanz-Puente, I.; Redondo-Salvo, S.; Torres-Cortés, G.; De Toro, M.; Fernandes, S.; Börner, A.; Lorenzo, Ó.; de la Cruz, F.; Robledo, M. Seed-mediated vertical transmission of *Pantoea* core endophytes. *ISME J.* **2025**, *19*, wraf192. [CrossRef]
4. Lopes, R.; Tsui, S.; Gonçalves, P.J.R.O.; De Queiroz, M.V. A look into a multifunctional toolbox: Endophytic *Bacillus* species provide broad and underexploited benefits for plants. *World J. Microbiol. Biotechnol.* **2018**, *34*, 94. [CrossRef]
5. Pitzschke, A. Developmental Peculiarities and Seed-Borne Endophytes in Quinoa: Omnipresent, Robust Bacilli Contribute to Plant Fitness. *Front. Microbiol.* **2016**, *7*, 2. [CrossRef]
6. Saxena, A.K.; Kumar, M.; Chakdar, H.; Anuroopa, N.; Bagyaraj, D.J. *Bacillus* species in soil as a natural resource for plant health and nutrition. *J. Appl. Microbiol.* **2020**, *128*, 1583–1594. [CrossRef]
7. Etesami, H.; Jeong, B.R.; Glick, B.R. Potential use of *Bacillus* spp. as an effective biostimulant against abiotic stresses in crops—A review. *Curr. Res. Biotechnol.* **2023**, *5*, 100128. [CrossRef]
8. Valencia-Marin, M.F.; Chávez-Avila, S.; Guzmán-Guzmán, P.; Orozco-Mosqueda, M.D.C.; De Los Santos-Villalobos, S.; Glick, B.R.; Santoyo, G. Survival strategies of *Bacillus* spp. in saline soils: Key factors to promote plant growth and health. *Biotechnol. Adv.* **2024**, *70*, 108303. [CrossRef]
9. Dimkić, I.; Janakiev, T.; Petrović, M.; Degrassi, G.; Fira, D. Plant-associated *Bacillus* and *Pseudomonas* antimicrobial activities in plant disease suppression via biological control mechanisms—A review. *Physiol. Mol. Plant Pathol.* **2022**, *117*, 101754. [CrossRef]
10. Fira, D.; Dimkić, I.; Berić, T.; Lozo, J.; Stanković, S. Biological control of plant pathogens by *Bacillus* species. *J. Biotechnol.* **2018**, *285*, 44–55. [CrossRef]
11. Kiesewalter, H.T.; Lozano-Andrade, C.N.; Wibowo, M.; Strube, M.L.; Maróti, G.; Snyder, D.; Jørgensen, T.S.; Larsen, T.O.; Cooper, V.S.; Weber, T.; et al. Genomic and Chemical Diversity of *Bacillus subtilis* Secondary Metabolites against Plant Pathogenic Fungi. *mSystems* **2021**, *6*, e00770-20. [CrossRef]
12. Shafi, J.; Tian, H.; Ji, M. *Bacillus* species as versatile weapons for plant pathogens: A review. *Biotechnol. Biotechnol. Equip.* **2017**, *31*, 446–459. [CrossRef]
13. Chen, W.; Zhu, B.; Yang, C.; Wei, C.; He, Y.; Zheng, L.; Liu, X.; Yang, J.; Tedersoo, L.; Lu, X.; et al. Decoupling Responses of Phyllosphere and Rhizosphere Bacterial Communities to Spatiotemporal Environmental Changes. *Glob. Change Biol.* **2025**, *31*, e70175. [CrossRef]
14. Liu, S.; He, F.; Kuzyakov, Y.; Xiao, H.; Hoang, D.T.T.; Pu, S.; Razavi, B.S. Nutrients in the rhizosphere: A meta-analysis of content, availability, and influencing factors. *Sci. Total Environ.* **2022**, *826*, 153908. [CrossRef]
15. Arnaouteli, S.; Bamford, N.C.; Stanley-Wall, N.R.; Kovács, Á.T. *Bacillus subtilis* biofilm formation and social interactions. *Nat. Rev. Microbiol.* **2021**, *19*, 600–614. [CrossRef]
16. Murugan, P.A.; Sahu, M.K.; Gupta, M.K.; Sankar, T.S.; Chandran, S.; Matheshwaran, S. Deciphering the influence of NaCl on social behaviour of *Bacillus subtilis*. *R. Soc. Open Sci.* **2024**, *11*, 240822. [CrossRef]
17. Rosazza, T.; Earl, C.; Eigentler, L.; Davidson, F.A.; Stanley-Wall, N.R. Reciprocal sharing of extracellular proteases and extracellular matrix molecules facilitates *Bacillus subtilis* biofilm formation. *Mol. Microbiol.* **2024**, *122*, 184–200. [CrossRef]
18. Zaidi-Ait Salem, M.; Nait Chabane, Y.; Girbal-Neuhauser, E. Architecture and physico-chemical properties of *Bacillus amyloliquefaciens* L-17 pellicle formed at the air–liquid interface. *J. Biosci. Bioeng.* **2021**, *132*, 560–568. [CrossRef]
19. Zhang, Y.; Silva, D.M.; Young, P.; Traini, D.; Li, M.; Ong, H.X.; Cheng, S. Understanding the effects of aerodynamic and hydrodynamic shear forces on *Pseudomonas aeruginosa* biofilm growth. *Biotechnol. Bioeng.* **2022**, *119*, 1483–1497. [CrossRef]
20. Muhammad, M.H.; Idris, A.L.; Fan, X.; Guo, Y.; Yu, Y.; Jin, X.; Qiu, J.; Guan, X.; Huang, T. Beyond Risk: Bacterial Biofilms and Their Regulating Approaches. *Front. Microbiol.* **2020**, *11*, 928. [CrossRef]
21. Stoll, A.; Salvatierra-Martínez, R.; González, M.; Araya, M. The Role of Surfactin Production by *Bacillus velezensis* on Colonization, Biofilm Formation on Tomato Root and Leaf Surfaces and Subsequent Protection (ISR) against *Botrytis cinerea*. *Microorganisms* **2021**, *9*, 2251. [CrossRef]
22. Stannius, R.O.; Fusco, S.; Cowled, M.; Kovács, Á.T. Surfactin accelerates *Bacillus subtilis* pellicle biofilm development. *Biofilm* **2024**, *9*, 100249. [CrossRef]
23. Schenk, H.J.; Espino, S.; Romo, D.M.; Nima, N.; Do, A.Y.T.; Michaud, J.M.; Papahadjopoulos-Sternberg, B.; Yang, J.; Zuo, Y.Y.; Steppe, K.; et al. Xylem Surfactants Introduce a New Element to the Cohesion-Tension Theory. *Plant Physiol.* **2017**, *173*, 1177–1196. [CrossRef]
24. Khait, I.; Lewin-Epstein, O.; Sharon, R.; Saban, K.; Goldstein, R.; Anikster, Y.; Zeron, Y.; Agassy, C.; Nizan, S.; Sharabi, G.; et al. Sounds emitted by plants under stress are airborne and informative. *Cell* **2023**, *186*, 1328–1336.e10. [CrossRef]
25. Hussain, S.; Tai, B.; Ali, M.; Jahan, I.; Sakina, S.; Wang, G.; Zhang, X.; Yin, Y.; Xing, F. Antifungal potential of lipopeptides produced by the *Bacillus siamensis* Sh420 strain against *Fusarium graminearum*. *Microbiol. Spectr.* **2024**, *12*, e04008-23. [CrossRef]

26. Yuan, Q.; Yang, P.; Liu, Y.; Tabl, K.M.; Guo, M.; Zhang, J.; Wu, A.; Liao, Y.; Huang, T.; He, W. Iturin and fengycin lipopeptides inhibit pathogenic *Fusarium* by targeting multiple components of the cell membrane and their regulative effects in wheat. *J. Integr. Plant Biol.* **2025**, *67*, 2184–2197. [CrossRef]
27. Castaldi, S.; Petrillo, C.; Donadio, G.; Piaz, F.D.; Cimmino, A.; Masi, M.; Evidente, A.; Isticato, R. Plant Growth Promotion Function of Bacillus sp. Strains Isolated from Salt-Pan Rhizosphere and Their Biocontrol Potential against *Macrophomina phaseolina*. *Int. J. Mol. Sci.* **2021**, *22*, 3324. [CrossRef]
28. Thérien, M.; Kiesewalter, H.T.; Auria, E.; Charron-Lamoureux, V.; Wibowo, M.; Maróti, G.; Kovács, Á.T.; Beauregard, P.B. Surfactin production is not essential for pellicle and root-associated biofilm development of *Bacillus subtilis*. *Biofilm* **2020**, *2*, 100021. [CrossRef]
29. Shahid, I.; Han, J.; Hanooq, S.; Malik, K.A.; Borchers, C.H.; Mehnaz, S. Profiling of Metabolites of *Bacillus* spp. and Their Application in Sustainable Plant Growth Promotion and Biocontrol. *Front. Sustain. Food Syst.* **2021**, *5*, 605195. [CrossRef]
30. Andrić, S.; Meyer, T.; Ongena, M. *Bacillus* Responses to Plant-Associated Fungal and Bacterial Communities. *Front. Microbiol.* **2020**, *11*, 1350. [CrossRef]
31. Alvarez, F.; Castro, M.; Príncipe, A.; Borioli, G.; Fischer, S.; Mori, G.; Jofré, E. The plant-associated *Bacillus amyloliquefaciens* strains MEP218 and ARP23 capable of producing the cyclic lipopeptides iturin or surfactin and fengycin are effective in biocontrol of sclerotinia stem rot disease: Biocontrol of sclerotinia stem rot of soybean. *J. Appl. Microbiol.* **2012**, *112*, 159–174. [CrossRef]
32. Arnaouteli, S.; MacPhee, C.E.; Stanley-Wall, N.R. Just in case it rains: Building a hydrophobic biofilm the *Bacillus subtilis* way. *Curr. Opin. Microbiol.* **2016**, *34*, 7–12. [CrossRef]
33. Hobley, L.; Ostrowski, A.; Rao, F.V.; Bromley, K.M.; Porter, M.; Prescott, A.R.; MacPhee, C.E.; van Aalten, D.M.F.; Stanley-Wall, N.R. BslA is a self-assembling bacterial hydrophobin that coats the *Bacillus subtilis* biofilm. *Proc. Natl. Acad. Sci. USA* **2013**, *110*, 13600–13605. [CrossRef]
34. Kobayashi, K.; Iwano, M. BslA(YuaB) forms a hydrophobic layer on the surface of *Bacillus subtilis* biofilms. *Mol. Microbiol.* **2012**, *85*, 51–66. [CrossRef]
35. Ongena, M.; Jourdan, E.; Adam, A.; Paquot, M.; Brans, A.; Joris, B.; Arpigny, J.; Thonart, P. Surfactin and fengycin lipopeptides of *Bacillus subtilis* as elicitors of induced systemic resistance in plants. *Environ. Microbiol.* **2007**, *9*, 1084–1090. [CrossRef]
36. Veening, J.; Igoshin, O.A.; Eijlander, R.T.; Nijland, R.; Hamoen, L.W.; Kuipers, O.P. Transient heterogeneity in extracellular protease production by *Bacillus subtilis*. *Mol. Syst. Biol.* **2008**, *4*, 184. [CrossRef]
37. Schaeffer, A.B.; Fulton, M.D. A Simplified Method of Staining Endospores. *Science* **1933**, *77*, 194. [CrossRef]
38. Morris, L.S.; Evans, J.; Marchesi, J.R. A robust plate assay for detection of extracellular microbial protease activity in metagenomic screens and pure cultures. *J. Microbiol. Methods* **2012**, *91*, 144–146. [CrossRef]
39. Bonebrake, M.; Anderson, K.; Valiente, J.; Jacobson, A.; McLean, J.E.; Anderson, A.; Britt, D.W. Biofilms Benefiting Plants Exposed to ZnO and CuO Nanoparticles Studied with a Root-Mimetic Hollow Fiber Membrane. *J. Agric. Food Chem.* **2018**, *66*, 6619–6627. [CrossRef]
40. Płaza, G.; Chojniak, J.; Rudnicka, K.; Paraszkiewicz, K.; Bernat, P. Detection of biosurfactants in *Bacillus* species: Genes and products identification. *J. Appl. Microbiol.* **2015**, *119*, 1023–1034. [CrossRef]
41. Frank, J.A.; Reich, C.I.; Sharma, S.; Weisbaum, J.S.; Wilson, B.A.; Olsen, G.J. Critical Evaluation of Two Primers Commonly Used for Amplification of Bacterial 16S rRNA Genes. *Appl. Environ. Microbiol.* **2008**, *74*, 2461–2470. [CrossRef]
42. Vlamakis, H.; Chai, Y.; Beauregard, P.; Losick, R.; Kolter, R. Sticking together: Building a biofilm the *Bacillus subtilis* way. *Nat. Rev. Microbiol.* **2013**, *11*, 157–168. [CrossRef]
43. Lopez, D.; Vlamakis, H.; Kolter, R. Biofilms. *Cold Spring Harb. Perspect. Biol.* **2010**, *2*, a000398. [CrossRef]
44. Zhang, N.; Wang, Z.; Shao, J.; Xu, Z.; Liu, Y.; Xun, W.; Miao, Y.; Shen, Q.; Zhang, R. Biocontrol mechanisms of *Bacillus*: Improving the efficiency of green agriculture. *Microb. Biotechnol.* **2023**, *16*, 2250–2263. [CrossRef]
45. Rychel, K.; Sastry, A.V.; Palsson, B.O. Machine learning uncovers independently regulated modules in the *Bacillus subtilis* transcriptome. *Nat. Commun.* **2020**, *11*, 6338. [CrossRef]
46. Wei, X.; Pan, Z.; Chen, Z.; He, N. Stress response regulation to extracellular polymeric substances biosynthesis in *Bacillus licheniformis*. *Microb. Cell Factories* **2025**, *24*, 222. [CrossRef]
47. Huang, Q.; Zhang, Z.; Liu, Q.; Liu, F.; Liu, Y.; Zhang, J.; Wang, G. SpoVG is an important regulator of sporulation and affects biofilm formation by regulating Spo0A transcription in *Bacillus cereus* 0–9. *BMC Microbiol.* **2021**, *21*, 172. [CrossRef]
48. Markelova, N.; Chumak, A. Antimicrobial Activity of *Bacillus* Cyclic Lipopeptides and Their Role in the Host Adaptive Response to Changes in Environmental Conditions. *Int. J. Mol. Sci.* **2025**, *26*, 336. [CrossRef]
49. Soriano-Peña, E.Y.; Luna-Bulbarela, A.; Cristiano-Fajardo, S.A.; Galindo, E.; Serrano-Carreón, L. Modulation of the Sporulation Dynamics in the Plant-Probiotic *Bacillus velezensis* 83 via Carbon and Quorum-Sensing Metabolites. *Probiotics Antimicrob. Proteins* **2025**, *17*, 3743–3762. [CrossRef]

50. Bromley, K.M.; Morris, R.J.; Hobley, L.; Brandani, G.; Gillespie, R.M.C.; McCluskey, M.; Zachariae, U.; Marenduzzo, D.; Stanley-Wall, N.R.; MacPhee, C.E. Interfacial self-assembly of a bacterial hydrophobin. *Proc. Natl. Acad. Sci. USA* **2015**, *112*, 5419–5424. [CrossRef]
51. Earl, C.; Arnaouteli, S.; Bamford, N.C.; Porter, M.; Sukhodub, T.; MacPhee, C.E.; Stanley-Wall, N.R. The majority of the matrix protein TapA is dispensable for *Bacillus subtilis* colony biofilm architecture. *Mol. Microbiol.* **2020**, *114*, 920–933. [CrossRef] [PubMed]
52. Raaijmakers, J.M.; De Bruijn, I.; Nybroe, O.; Ongena, M. Natural functions of lipopeptides from *Bacillus* and *Pseudomonas*: More than surfactants and antibiotics. *FEMS Microbiol. Rev.* **2010**, *34*, 1037–1062. [CrossRef] [PubMed]
53. Flemming, H.C.; Wingender, J. The biofilm matrix. *Nat. Rev. Microbiol.* **2010**, *8*, 623–633. [CrossRef]
54. Ahlawat, O.P.; Yadav, D.; Kashyap, P.L.; Khippal, A.; Singh, G. Wheat endophytes and their potential role in managing abiotic stress under changing climate. *J. Appl. Microbiol.* **2022**, *132*, 2501–2520. [CrossRef]
55. Kuźniar, A.; Włodarczyk, K.; Grządziel, J.; Woźniak, M.; Furtak, K.; Gałązka, A.; Dziadczyk, E.; Skórzyńska-Polit, E.; Wolińska, A. New Insight into the Composition of Wheat Seed Microbiota. *Int. J. Mol. Sci.* **2020**, *21*, 4634. [CrossRef]
56. Mwita, L.; Chan, W.Y.; Pretorius, T.; Lyantagaye, S.L.; Lapa, S.V.; Avdeeva, L.V.; Reva, O.N. Gene expression regulation in the plant growth promoting *Bacillus atrophaeus* UCMB-5137 stimulated by maize root exudates. *Gene* **2016**, *590*, 18–28. [CrossRef]
57. Akram, W.; Waqar, S.; Hanif, S.; Anjum, T.; Aftab Ze, H.; Li, G.; Ali, B.; Rizwana, H.; Hassan, A.; Rehman, A.; et al. Comparative Effect of Seed Coating and Biopriming of *Bacillus aryabhattai* Z-48 on Seedling Growth, Growth Promotion, and Suppression of Fusarium Wilt Disease of Tomato Plants. *Microorganisms* **2024**, *12*, 792. [CrossRef] [PubMed]
58. Rocha, I.; Ma, Y.; Souza-Alonso, P.; Vosátka, M.; Freitas, H.; Oliveira, R.S. Seed Coating: A Tool for Delivering Beneficial Microbes to Agricultural Crops. *Front. Plant Sci.* **2019**, *10*, 1357. [CrossRef]
59. Kloepper, J.W.; Ryu, C.M.; Zhang, S. Induced Systemic Resistance and Promotion of Plant Growth by *Bacillus* spp. *Phytopathology* **2004**, *94*, 1259–1266. [CrossRef]